An Interdisciplinary Response to Mine Water Challenges - Sui, Sun & Wang (eds)
©2014 China University of Mining and Technology Press, Xuzhou, ISBN 978-7-5646-2437-8

Water Content Estimation of Aquifer Using Transient Electromagnetic Method

Bo Wang[1,2], Shengdong Liu[1,2], Zhichao Hao[2], Xiayang Zhang[1]
1 China University of Mining & Technology, wbsyes@126.com;
2 Anhui Huizhou Institute of Subterranean Calamity, 317987823@qq.com

Abstract Mine water is a menace to coal mining. Transient Electromagnetic Method (TEM) is a relatively quick and efficient method to detect the water yield property of a targeted layer. Based on mine-oriented 3D TEM observing system, the signal of induced voltage is obtained. TEM 3D data volume can be calculated through the calculation of late-period resistivity and time-depth conversion. After setting an appropriate apparent resistivity value, we can determine the spatial distribution range of an aquifer. Then, combined with water-filling coefficient of the aquifer, its water content can be finally estimated. The water yield property detection in the No.4 coal seam goaf of 80101 workface in Jude mine of Shanxi, China, demonstrates that the apparent resistivity of this goaf is lower than 3 Ω·m, and the projection area of low-resistivity anomaly zone amounts to 22,383 m^2. Given by the formula *Q=KMS*, we can estimate the water volume as 33,574 m^3. Three boreholes have been constructed for the later dredging and drainage project, which results in a total water yield of 36,774 m^3, thus the error percentage of the predicted water yield is 8.7%. So it can be concluded that it is feasible to predict aquifer's water content with TEM method.
Keywords water content estimation, transient electromagnetic method, apparent resistivity, qoaf

Introduction

Based on TEM method, ungrounded loop-line and grounding electrode can tansmit down pulse-type primary field, which may induce an eddy current, and then the spatial and temporal distribution of secondary field caused by the eddy current can be observed by coil and grounding electrode (Yu 2007; Liu et al. 2009; Jiang et al. 2010; Wang et al. 2012). From Fig.1 it can be seen that, TEM receives induced signals during the time-off period, which will be attenuated over time.

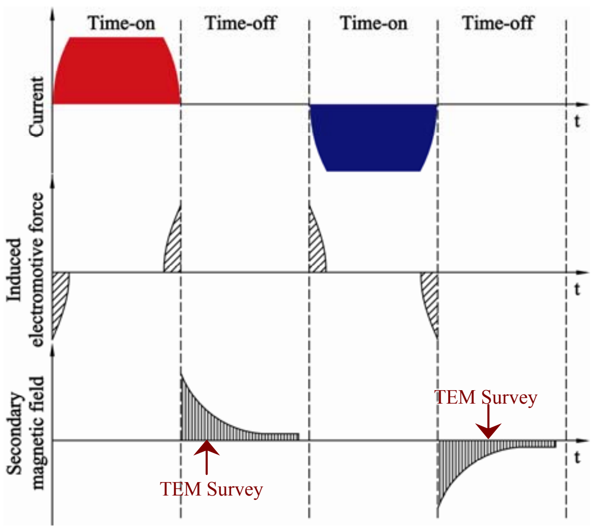

Fig .1 *Sketch map of primary and secondary field*

By TEM method, we can solve some geological problems. Featuring light equipment, little lateral influence, and high resolution, this method can be widely applied in water disaster prevention and control. However, in the case of theory and processing software restraints, the analyses are usually qualitative, which cannot meet the standard of quantification, and, to certain extent, hold up its wider application [Tao 2009; Huang 2010; Xu2012]. Thus, this paper will create a theory and a method to calculate TEM response by means of equivalent substitution, interpret the diffusion law of TEM field from the perspective of physics, calculate physical parameters, and conduct 3D apparent resistivity imaging and quantitative analyses of detection results.

TEM Data Processing

Apparent resistivity calculation

Currently, for mine-oriented small multi-turn loop device, apparent resistivity is mostly calculated by general reduction formula of early/late time apparent resistivity. For example, the late-time apparent resistivity is still calculated by the classical half-space homogeneous field late-time formula:

$$\rho_t = \frac{C\mu_0}{4\pi t}[\frac{2\mu_0 SNsn}{5t(V/I)}]^{2/3} = C \times 6.32 \times 10^{-12} \times (S \times N)^{2/3} \times (s \times n)^{2/3} \times (V/I)^{-2/3} \times t^{-5/3} \quad (1)$$

Where ρ_t denotes apparent resistivity, and μ_0 represents vacuum permeability. *S* is single-turn transmitting loop area, while *s* denotes single-turn receiving loop area, and both of their units are m^2. *N* and *n* are respectively the turns of transmitting and receiving coil. *V* denotes induced electromotive force and current, whose unit is *V*, and *I* represents current, whose unit is A. *V/I* is the received normalized value of secondary induction field. *t* is the observing time for secondary field attenuation, its unit being s, and *C* is approximation coefficient.

Depth conversion

The detection depth of the TEM method is related to transmitting magnetic torque, overlayer resistivity, and the minimal resolutive voltage. The time-depth conversion equation for mine-oriented TEM method is:

$$V_s = \alpha \frac{\rho_s \sqrt{\gamma\pi}}{\mu\alpha}\{C_1 + (C_1^2)^{1/2} + [1 + \frac{C_1}{(C_1^2+2)^{1/2}}]\gamma C_2\} \quad (2)$$

$$D = V_S \times t_i \quad (3)$$

Where α is conversion coefficient, which is relative to the heterogenous conductor in the vicinity of roadway, usually values between 0.6 and 1.8. β is the factor of proportionality. $\gamma = \mu\alpha^2/(4\rho_i t_i)$, where ρ_i is the corresponding resistivity value of moment t_i.

$$C_1(\gamma) = \frac{3\sqrt{\pi}}{4}[1 - \frac{\gamma}{4} - \sum_{k=1}^{\infty}\frac{(2k-3)!!}{k!(k+1)!}(\frac{\gamma}{2})^k] \quad (4)$$

$$C_2(\gamma) = \frac{3\sqrt{\pi}}{4}[1 - \frac{\gamma}{4} - \sum_{k=0}^{\infty}\frac{(2k-1)!!}{k!(k+1)!}(\frac{\gamma}{2})^k] \quad (5)$$

The completion of apparent resistivity calculation and depth conversion will lead to the contour map making. Kriging algorithm is used for data interpolation, while natural zero method can be useful with regard to sectorial data volume.

3D slice extraction

3D visualization is a technique to reveal and describe spatial data, and to receive the subsurface geological structure and features, which provides information for accurate description of 3D geological structure, and facilitates the exploration and development of coal mine.

According to data combinations received from different detection directions, 3D visualization can clearly display the spatial distribution of anomalies with different resistivity values correspond to different threshold values, the scattered points, and the range of apparent resistivity. However, a cross-section map can be clearer in showing the anomaly areas at a specific depth on a profile. Cross-sections can be extracted from different depths of plane XY, YZ, and ZX. Apparent resistivity data can be extracted at any depth, or any vertical profile.

Estimation of aquifer's water content

Utilizing the cross-section map, the aquifer water volume can be calculated by the following formula:

$$Q=KMS \tag{6}$$

Where Q is aquifer water content, K the water containing coefficient, M the aquifer thickness, and S the water-rich area in aquifer.

Water yield property survey in a mine goaf

Geological settings

The No.80101 workface of Jude mine in Shanxi Province occurs under L1 limestone in the middle and lower part of Taiyuan Formation, 60.6 m beneath the 4# seam. The seam occurrence is stable with a thickness range of 1.8 to 3.2 m, and a 2.8 m thickness on average. Part of the area contains a 0.05 to 0.1 m dirt band of mudstone or carbonolite (carbonaceous mudstone). At the bottom of the seam is a pyrite seam in forms of lamella and nodule.

Field detection

In order to detect the spatial distribution of goaf and estimate the water volume, MTEM was adopted with the YCS360 Electromagnetic System. The detection onset of workface No.80101 (as shown in fig.2) is at the intersection of the return airway and the concentrated rail roadway, from return airway through open-off cut, and ends at the intersection of intake airway and concentrated rail roadway, with a detection workload of 3470 m in total, including 1660 m along the return airway, 150 m of open-off cut, and 1660 m along intake airway. Monitoring points are set every 10 meters, and the detection is conducted in 6 directions, respectively, 60°, 45°, and 30° to the external wall roof, normal to the roof, 30° and 45° to the internal wall roof.

Data interpretation and result analysis

The data interpretation is carried out from the perspective of geophysical characteristics, and the features are shown in 3D images. Water content is higher in the areas where the fractures are concentrated in the aquifer, manifesting as higher electrical conductivity and lower resistivity (i.e., high potential-low resistivity) anomalies. This characteristic identifies aquifer areas as those where the roof resistivity is lower than 3 Ω·m.

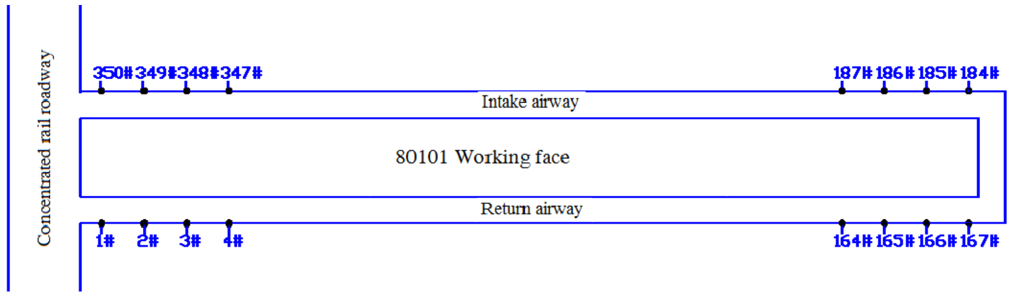

Fig. 2 *Arrangement diagram of MTEM*

Fig.3 is a 3D spatial distribution graph of anomalies at different depths above the No.80101 workface. 40 meters above the roof is a water-rich strata, and key preventions should be focused on region YC1, YC7, YC10. Anomaly area YC7 is located from 1085 m to 1850 m along the return airway (between monitoring point KF13 to KF15), 0-120 m along the inclination slope(120 m within return airway and workface), and 40 m to 60 m above the roof(more details seen in Fig.1), with an anomaly-impacted area of 22,383 m^2. According to $Q=KMS$, the goaf water-filling coefficient is 0.25 to 0.35, while the detection result of the actual coefficient is 0.3. It is indicated by the effect sketch that M is 5m, and thus we can deduce Q=33,574 m^3. Verification of the calculated values based on field measurements is shown in Table 1.

Conclusion

TEM resistivity imaging boasts rapid imaging, high quantification level, and high resolution, especially, for low resistivity body with a high-resistivity overlayer. Calculating the projection area S of low-resistivity anomaly zone, combining water containing coefficient K with aquifer thickness M, the aquifer water content can be estimated, with the error percentage of the predicted water yield below 9%. TEM 3D presentation and analysis provide a new method for estimation of water content in aquifer.

References

Jiang ZH, Yue JH, Yu JC (2010) Experiment in metal disturbance during advanced detection using a transient electromagnetic method in coal mines. J Mining Science and Technology 20: 861-863

Jia KH, Ju ZD, Qing CL, Shang PX, Hui C (2010) Application research of transient electromagnetic method in the underwater-karst detection. In: Chinese Geophysical Society, Chengdu, China, The 4th International Conference on Environmental and Engineering Geophysics, Chengdu University of Technology 555-559

Liu ZX, Liu SC, Liu YG (2009) Research on Transient Electromagnetic field of mine water-bearing structure by physical model experiment. J Rock Mechanics and Engineering 28: 259-266

Tao WP, Dong SH, Wei JS, Liu XM (2009) Application of transient electromagnetic method in detecting mining area's transmissivity and water yield property. J Energy Technology and Management 3: 1-3

Wang B, Liu SD, Yang Z, Huang LY (2012) Fine analysis on advanced detection of transient electromagnetic method. J Mining Science and Technology 22: 669-673

Xu JP, Liu SD, Wang B (2012) Electrical monitoring criterion for water flow in faults activated by mining. J Mine Water and the Environment 31: 172-179

Yu JC, Liu ZX, Liu SC, Tany JY (2007) Theoretical analysis of mine transient electromagnetic method and its application in detecting water burst structures in deep coal stope. J China Coal Society 32: 818-821

Yu JC (2007) Mine transient electromagnetism prospecting – Vol 7, transient electromagnetism. China University of Mining and Technology Press, Xuzhou, 181

Yu JC, Liu ZX, Tang JY (2007) Research on full space transient electromagnetic technique for detecting aqueous structures in coal mines. J China University of Mining Technology 17: 58-62

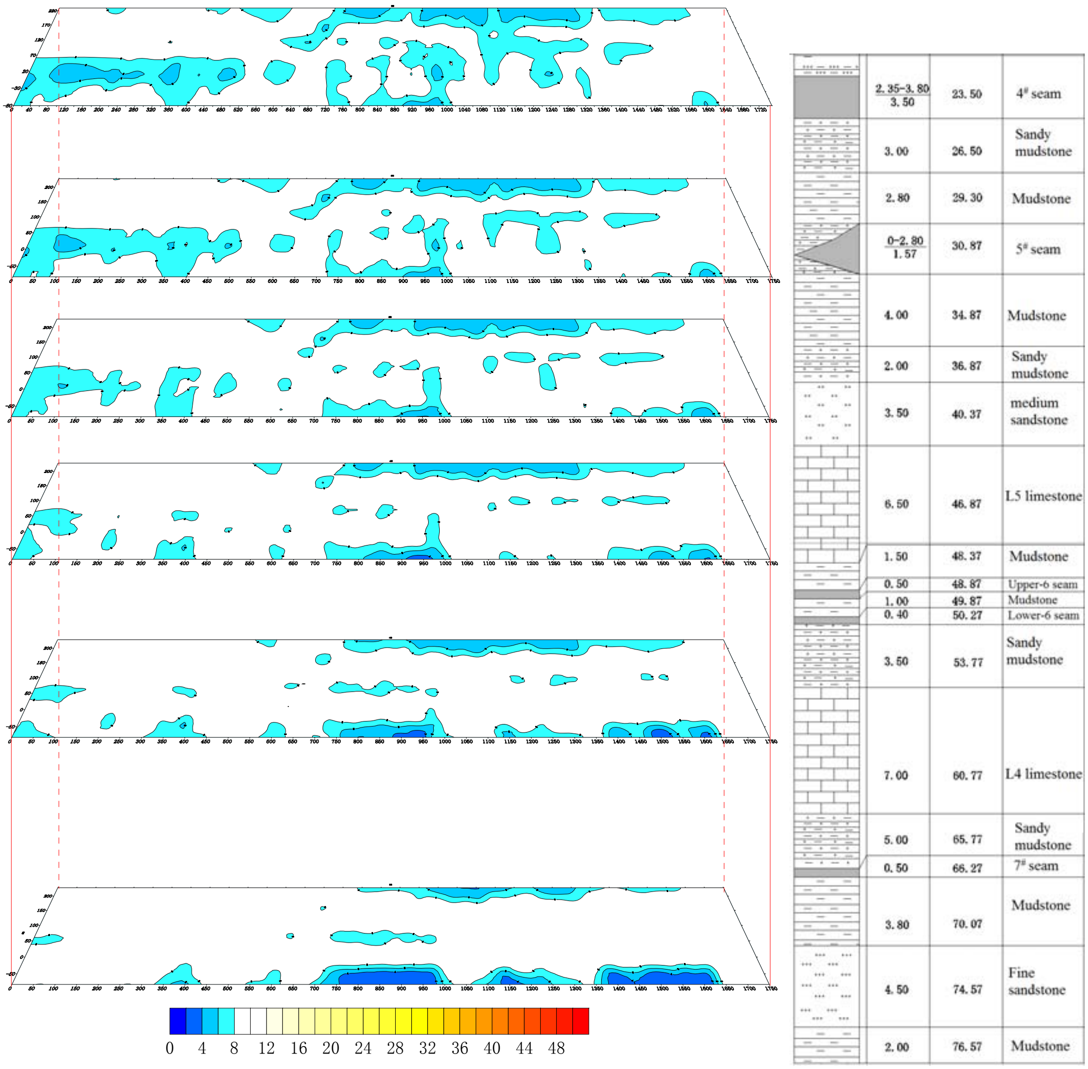

Fig .3 *The 3D spatial distribution of anomalies at different depths above the No.80101 workface*

***Table 1** Drilling log table of Anomaly YC7 in No.80101 workface*

Location	Drilling Log Number	Parameter			Final Hole Position	Hydrology	Source	Total Volume (m^3)
		Azimuth (°)	Dip (°)	Depth (m)				
No.18 drilling field of No.80101 return airway	H19-1	313	37	129	115m to 4# seam	water yield $8m^3/h$ at 60m	Limestone water above 8# seam	3,685
	H19-2	277	46	125	90m to 4# goaf	Water yield $30m^3/h$ from final hole	Goaf water from 4# seam	15,267
	H19-3	221	41	130	95m to 4# goaf	Water yield $35m^3/h$ from final hole	Goaf water from 4# seam	12,379
	H19-4	136	36	157	99m to 4# goaf	none	/	/
	H19-5	237	-1	141	Floor of 8# seam	none	/	/
	H19-6	221	1	132	Floor of 8# seam	none	/	/
	H19-7	229	-10	130	Floor of 8# seam	none	/	/
	H19-S1	238	35	111	4# seam	Water yield $3m^3/h$ from final hole	Goaf water from 4# seam	5,443
	H19-S2	308	30	156	109m to 4# goaf	none	/	/